213+120 FAST REACTOR 1450
7/8/70 A+B Irrad

AI–AEC–12961

VOID FORMATION IN PROTON-IRRADIATED STAINLESS STEEL

AEC Research and Development Report

Atomics International
North American Rockwell

P.O. Box 309
Canoga Park, California 91304

P5909

DISCLAIMER

LEGAL NOTICE

Printed in the United States of America
Available from
Clearinghouse for Federal Scientific and Technical Information
National Bureau of Standards, U.S. Department of Commerce
Springfield, Virginia 22151
Price: Printed Copy $3.00; Microfiche $0.65

AI–AEC–12961
METALS, CERAMICS
AND MATERIALS

VOID FORMATION IN PROTON-IRRADIATED STAINLESS STEEL

By

D. W. KEEFER
H. H. NEELY
J. C. ROBINSON
A. G. PARD
D. KRAMER

Atomics International
North American Rockwell

P.O. Box 309
Canoga Park, California 91304

CONTRACT: AT(04-3)-824
ISSUED: JUNE 30, 1970

DISTRIBUTION

This report has been distributed according to the category "Metals, Ceramics and Materials" as given in the Standard Distribution for Unclassified Scientific and Technical Reports, TID-4500.

ACKNOWLEDGMENT

The authors express their sincere thanks to Mr. R.M. Kniefel and Mr. K. R. Garr for their able assistance in the initial phases of these experiments and for performing the helium injections.

CONTENTS

FIGURES

FIGURES

ABSTRACT

Voids have been produced by 1.2-MeV proton irradiation at 500°C in Type 316 stainless steel containing 2 atomic parts per million (appm) helium. The proton fluence was 6×10^{18} p/cm^2. Observation of electron microscope foils, obtained at various positions along the proton pathlength, has shown that the average void diameter increased with increasing number of atom displacements, but that the void density remained constant. Calculated volume swelling ranged from 0.2 to 5%, depending on the number of displacements. In addition to voids, irradiation-produced dislocation loops and small precipitate particles on dislocations have been observed.

THIS PAGE

WAS INTENTIONALLY

LEFT BLANK

I. INTRODUCTION

The first observation, in an irradiated metal, of what are now known to be voids was reported by Cawthorne and Fulton.[1] Other such observations followed, and it quickly became apparent that the occurrence of voids presented a significant practical problem related to the dimensional stability of various reactor components, notably fuel cladding.[2] The formation of voids also presents a tantalizing subject for basic studies of the behavior of radiation-produced point defects in metals, and some work on irradiated pure metals has been reported.[3]

Progress in achieving a detailed understanding of void formation has been relatively slow; the complexity of the process whereby voids nucleate and grow certainly accounts, in part, for this. Also, most studies have been performed on complex alloys, and control of important material properties has not always been possible. Perhaps most important, the majority of irradiations have been performed in reactors. Such irradiations necessitate long exposure times, and control and monitoring of specimen temperature and neutron flux and fluence are difficult. Further, helium and hydrogen are produced in significant quantities in many metals during reactor irradiations, and the importance of the presence of these impurities on void formation cannot be established.

As has already been demonstrated at Harwell, irradiation with heavy charged particles can also be used to form voids.[4] The British have successfully produced voids in stainless steel with protons, as well as with iron and carbon ions. There are a number of advantages to studying void formation in this way. All experimental conditions are far more easily controlled and monitored than in a reactor. Further, heavy charged particles, because of their higher displacement cross sections, compress the experimental time from the several years required in a reactor to a few hours in an accelerator. An additional advantage to the use of charged particles comes about because of the inverse relationship (for Rutherford scattering) between the displacement cross section and particle energy. As the particles slow down in their traversal of a specimen, the displacement rate and total number of displacements increase. Thus, information on voids produced under effectively different irradiation conditions at the same

temperature can be obtained from electron microscope foils taken from various positions within the thickness of a single specimen.

Although the production of voids by heavy charged-particle irradiation will undoubtedly be of great value in void studies, the precise correlation between void arrays created by neutrons and those produced by charged particles may require careful study. The difference in time scale of the two experimental techniques and variations in the nature of damage created by the different particles will have to be taken into account in such a correlation.

The present proton-irradiation experiments are intended to study the effects of atom displacement rate, total number of displacements, temperature, helium content, and microstructure on void formation and the attendant volume swelling in Type 316 stainless steel. It is also hoped that, out of this program, a correlation with reactor irradiations will be developed. Thus far, only preliminary irradiations have been made. Although voids have been produced, the results reported here must be viewed in the context of their preliminary nature.

II. EXPERIMENTAL PROCEDURE

A. SPECIMEN PREPARATION

The specimens used in this work are 0.0127-mm thick foils having cross-sectional dimensions of 1.78 by 0.88 cm. Following an appropriate heat treatment, the specimens are diffusion bonded, under pressure, to thick copper plates. These plates serve as a heat transfer medium between the specimens and the temperature-control apparatus.

Prior to irradiation, the specimens are injected with helium by means of a cyclotron. The procedures used here are similar to those employed previously by members of our laboratory, and result in an even distribution of helium throughout the sample volume.[5] The helium content is determined by mass spectrometry.[6] The temperature of samples undergoing helium injection does not rise significantly above ambient.

Following irradiation, the copper plate is removed from each specimen by immersion in nitric acid. Each specimen is then cut into at least six sections for electron microscope examination. Microscope foils are obtained from selected positions within the specimen thickness by means of careful electropolishing of a section. The polishing procedure is periodically interrupted so that X-ray absorption measurements can be made to monitor thickness, and hence the ultimate position from which the foil is obtained. It is estimated that the foil position, determined in this way, is accurate within ±2500 Å. This accuracy is to be improved upon in future experiments.

B. TARGET ASSEMBLY

The target assembly is shown in Figure 1. The main body of the assembly serves as a reservoir for cooling water. The three support posts of the specimen heater block are soft soldered to this reservoir. The block contains a coiled heater element. Bolting of the specimen plate to the heater block completes the heat transfer system.

C. TEMPERATURE CONTROL

During irradiation, the specimen temperature is monitored by an infrared detector which has previously been calibrated against a thermocouple attached

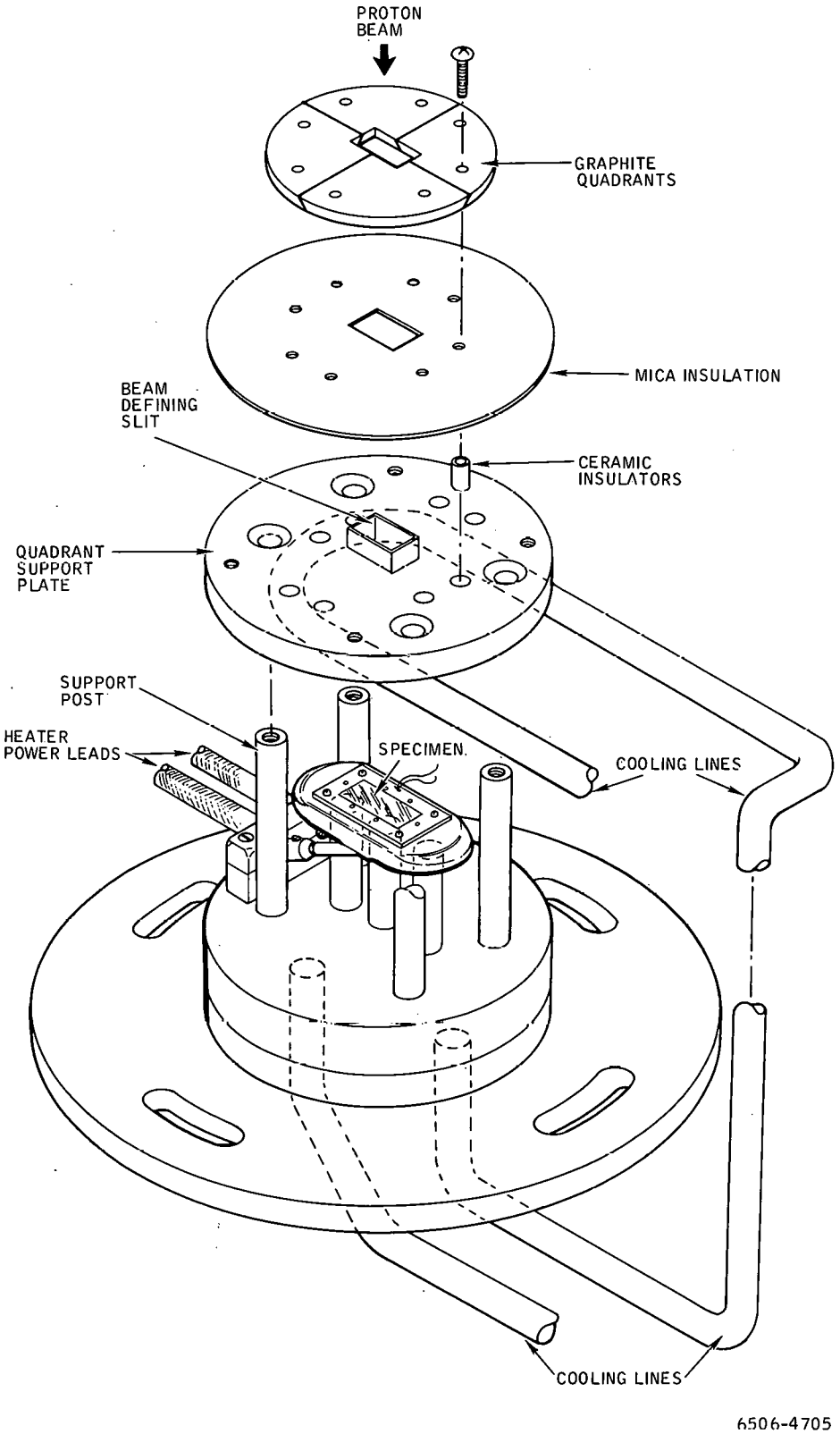

Figure 1. Exploded View of Proton-Irradiation Target Assembly

to the heater block. The output of the detector is also used in the programming circuit of an electronic temperature-control system. During an irradiation at 500°C with a 1.2-MeV beam of $\sim 1.6 \times 10^{15}$ p/cm^2-sec, the control system was able to keep the temperature typically within ±10°C. Extreme beam instability led to periodic fluctuations downward of ~20°C.

D. PROTON BEAM

The proton beam is delivered by a 3-MeV Dynamitron. The beam is magnetically analyzed, shaped, and steered prior to its entry into the target chamber. The shape and homogeneity of the beam is continuously observed by means of a High Voltage Engineering Corporation beam profile monitor. The particles emerging from the Dynamitron source are preponderantly Mass II particles (i.e., two protons with a shared electron). In order to achieve high proton beam currents, it is these Mass II particles which are made to impinge on the target. The energy required to separate each pair of protons from the electron is only a few eV, and the separation occurs at the specimen surface. Thus, no significant error in proton energy occurs with this technique. In this report, proton energies and currents are stated directly (e.g., a Mass II energy of 2.0 MeV and current of 1×10^{15} particles/cm^2-sec will be given as a proton energy of 1.0 MeV and a current of 2×10^{15} p/cm^2-sec).

The proton beam is defined, by a graphite quadrant system, to an area of 2.0 cm^2 (see Figure 1). This system is attached to a water-cooled support plate; this plate further defines the beam on the sample to an area of 1.3 cm^2. Each quadrant is electrically biased with respect to the target chamber in order to minimize back-scattered electrons. The proton current which is integrated is the sum of the currents measured on the specimen and the target chamber.

E. DISPLACEMENT CALCULATIONS

The total number of displacements created by a flux of protons, φ, in time, t, is given by

$$N = N_o \sigma_d \bar{\nu} \varphi t \quad , \qquad \ldots (1)$$

where:

N_o = number of atoms per unit volume

σ_d = displacement cross section for protons of a given energy

$\overline{\nu}$ = mean number of displacements created per primary knock-on.

The Kinchin-Pease model was used in calculating $\overline{\nu}$. σ_d and $\overline{\nu}$ have been determined as functions of proton energy, and, with appropriate values of φ and t, have been used in calculating the number of displacements and displacement rate as a function of proton penetration into a specimen. Proton energy loss, as a function of energy (i.e., depth of penetration), was obtained from Reference 7.

III. EXPERIMENTAL RESULTS

The data presented here were obtained from a single specimen of Type 316 stainless steel. Prior to bonding to its copper plate, the specimen was solution annealed at 980°C in vacuum for one hour. This was followed by an eight-hour precipitation anneal at 760°C. This treatment ("Treatment Number 6") results in the formation of $M_{23}C_6$ carbides at the austenite grain boundaries. The average grain size is between 20 and 30 μm. After the annealing treatment, the specimen was bonded to a copper plate and subsequently injected with helium to a level of 2 appm.

During irradiation, the specimen temperature was maintained at 500 ± 10°C, with periodic downward fluctuations of >10°C. The 1.2-MeV proton flux was nominally 1.6×10^{15} p/cm^2-sec; but, due to beam instability, the average flux was approximately half this value. The average flux has been used in all calculations. The fluence was $\sim 6 \times 10^{18}$ p/cm^2.

The range of a 1.2-MeV proton in stainless steel is 0.0084 mm.[7] Electron microscope foils were taken at proton penetration distances of 0.0025, 0.0051, and 0.0076 mm by the technique described in a preceding paragraph. Results from a foil produced prior to development of the X-ray absorption technique will also be discussed. Although the exact position of this foil is not known, the results clearly indicate that it was taken from a depth slightly beyond the 0.0076-mm level.

At the 0.0025-mm position, the energy of a 1.2-MeV incident proton has been reduced to 0.93 MeV. The displacement cross section at this energy is 3.4×10^{-20} cm^2, and $\bar{\nu}$ is ~4.1. The displacement rate at the 0.0025-mm position is, from Equation 1 with $\varphi \cong 8 \times 10^{14}$ p/cm^2-sec, $\sim 1 \times 10^{-4}$ atom fraction/sec. The total number of displacements is 7×10^{22}/cm^3.

Figure 2 shows the disposition of voids obtained at the 0.0025-mm position. Also visible in the photograph are faulted dislocation loops and other dislocation structure. Careful examination of the foil has revealed the presence of small precipitates on dislocations; these can be detected in Figure 2. These precipitates are not present in unirradiated material. A more detailed photograph, showing the orientation of the loops, is shown in Figure 3.

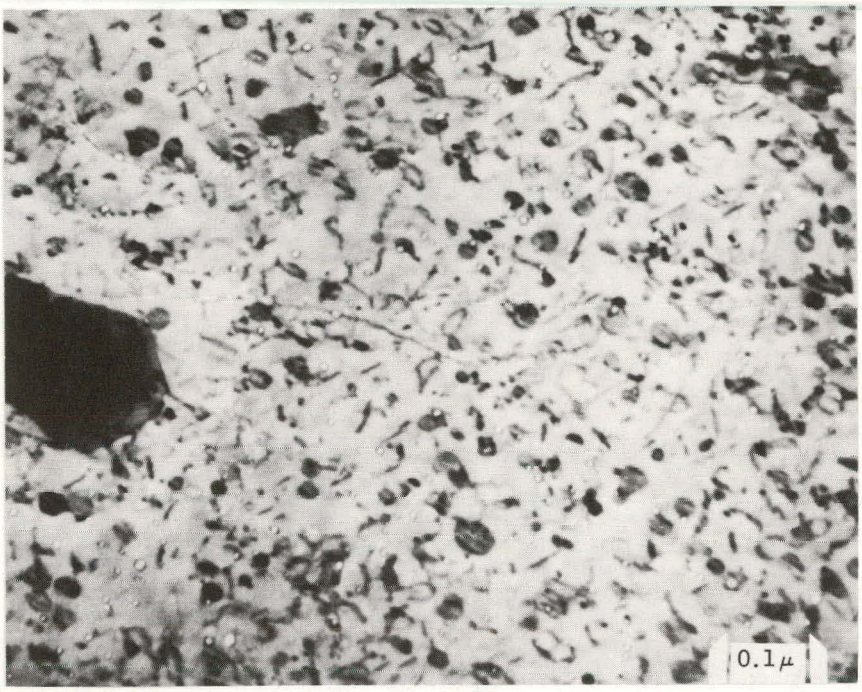

12-129

Figure 2. Transmission Electron Micrograph Showing Voids Obtained in Type 316 Stainless Steel Containing 2 appm Helium and Irradiated at 500°C. Proton penetration depth = 0.0025 mm. Note presence of faulted dislocation loops and dislocations decorated with small small precipitate particles.

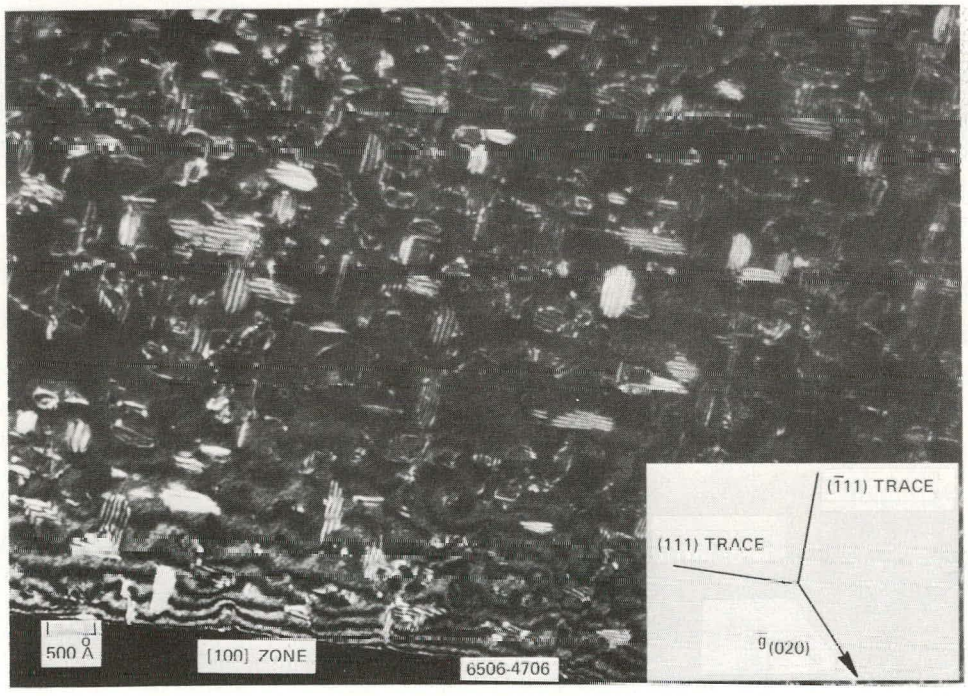

Figure 3. Transmission Electron Micrograph Showing Details of Dislocation Loops as Seen in Dark-Field Contrast. Proton penetration depth = 0.0025 mm.

The void number and size distribution were obtained by means of a Zeiss particle size analyzer. At the 0.0025-mm position, the void density was $\sim 3 \times 10^{15}$ voids/cm^3. The size distribution is shown as a histogram in Figure 4; the average void size in this distribution is ~110 Å. From the information in Figure 4, the swelling (increase in volume per unit volume) due to void formation is calculated to be 0.2%.

At the 0.0051-mm position, the proton energy has been reduced to 0.61 MeV, and the displacement cross section and $\bar{\nu}$ are $\sim 5.1 \times 10^{-20}$ cm^2 and 3.9, respectively. The displacement rate is $\sim 1.6 \times 10^{-4}$ atom fraction/sec, and the total number of displacements is 10^{23}/cm^3. The voids obtained at the 0.0051-mm level are shown in Figure 5. Faulted dislocation loops and dislocations decorated with small precipitates are also visible in the figure. The density of voids observed at this level was 10^{16}/cm^3. The size distribution is shown in Figure 6; the average void diameter in this distribution is 70 Å. The calculated volume swelling is 0.2%.

At the penetration distance of 0.0076 mm, the proton energy has been reduced to ~0.14 MeV. This corresponds to a cross section of 2.2×10^{-19} cm^2 and a $\bar{\nu}$ of 3.2. The displacement rate is $\sim 5.6 \times 10^{-4}$ atom fraction/sec, and the total number of displacements is 3.5×10^{23}/cm^3. The voids observed at the 0.0076-mm level are shown in Figure 7. The density of voids obtained from this photograph was $\sim 4.5 \times 10^{15}$/cm^3. The average void diameter, from the size distribution shown in Figure 8, is ~150 Å. The volume swelling is calculated to be ~1%.

As mentioned in a preceding paragraph, the exact position of the fourth foil is now known. Therefore, the defect production rate and total number of displacements cannot be calculated. However, because of the large amount of damage observed in this foil (see Figure 9), it appears that the foil position was beyond the 0.0076-mm depth. Note that the void density is homogeneous throughout the microstructure. Similar results have been obtained at the other sample positions. This observation is different from those made following reactor irradiations, where, along grain boundaries, zones denuded of voids have frequently been observed. From Figure 9, the void density is 3×10^{15}/cm^3. Trace analyses of the voids at this level in three orientations – [100], [110], [211] – have

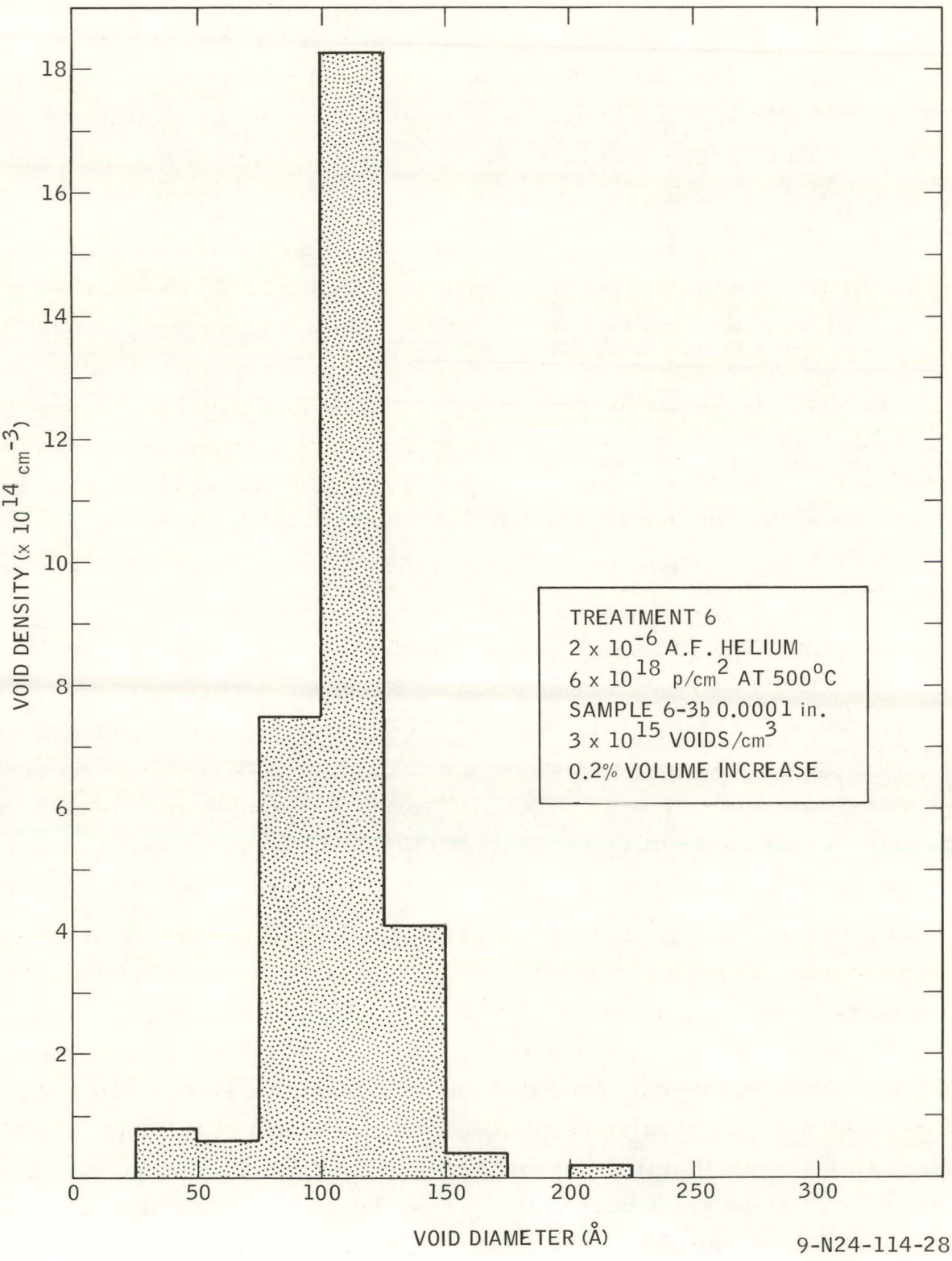

Figure 4. Histogram Showing Void-Size Distribution at 0.0025-mm Level. Average void size ~110 Å.

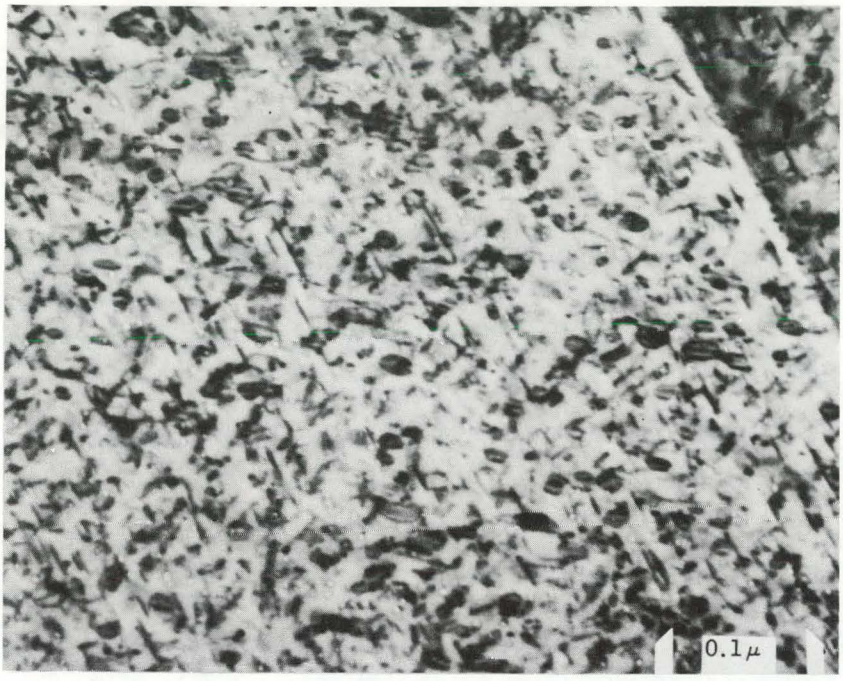

11-132

Figure 5. Transmission Electron Micrograph Showing Voids Obtained at a Proton Penetration Depth of 0.0051 mm in Type 316 Stainless Steel Containing 2 appm Helium

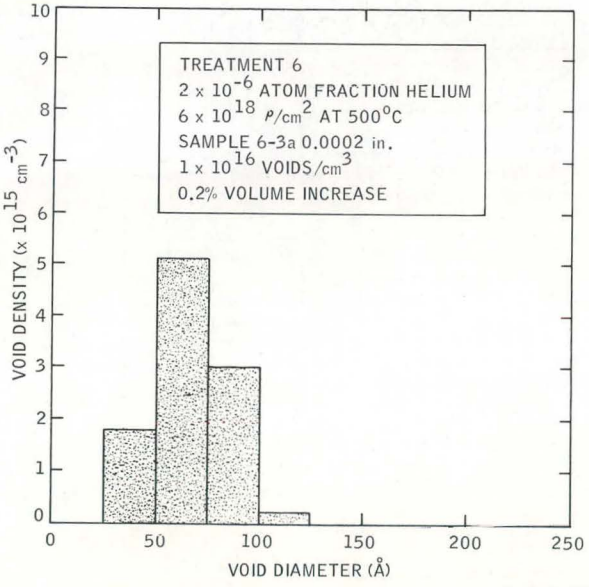

70-J27-007-35

Figure 6. Histogram Showing Void-Size Distribution at 0.0051-mm Level. Average void size ~70 Å.

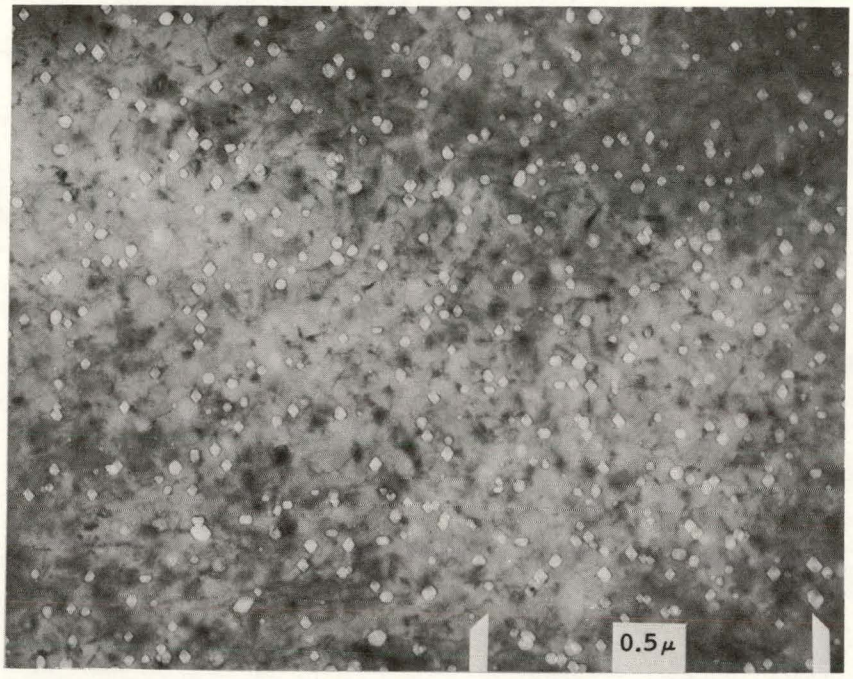

3-140

Figure 7. Transmission Electron Micrograph Showing Voids Obtained at a Proton Penetration Depth of 0.0076 mm in Type 316 Stainless Steel Containing 2 appm Helium

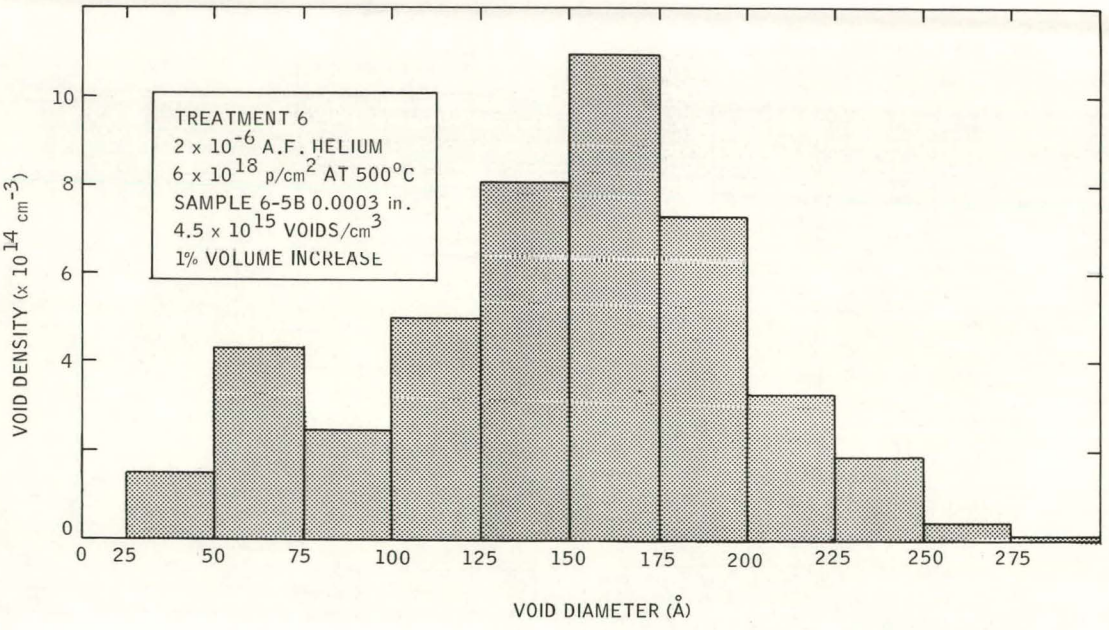

70-J27-007-34

Figure 8. Histogram Showing Void-Size Distribution at 0.0076-mm Level Average void size ~150 Å.

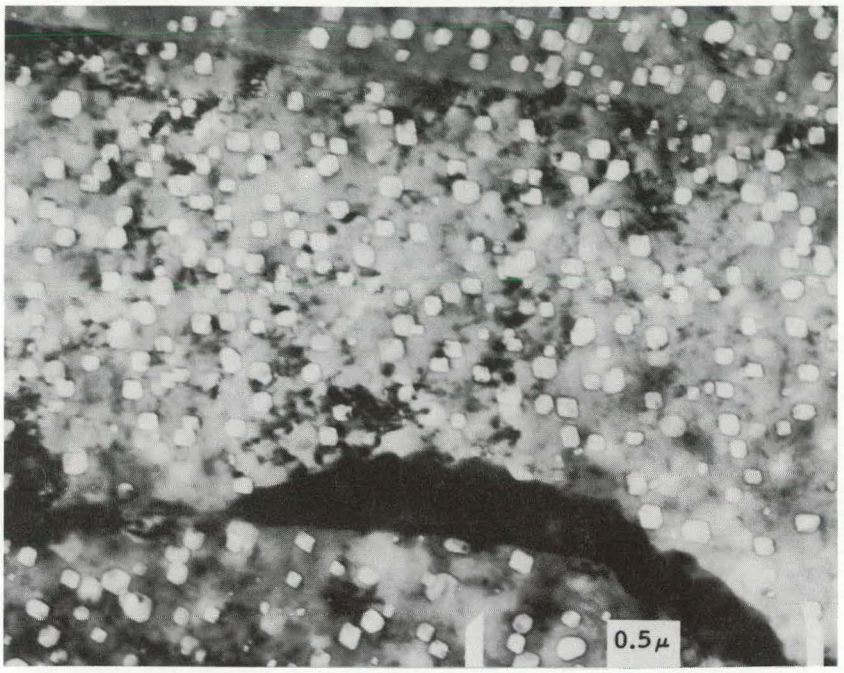

19-126

Figure 9. Transmission Electron Micrograph Showing Voids Obtained at a Proton Penetration Depth of >0.0076 mm. Note homogeneous void distribution throughout microstructure.

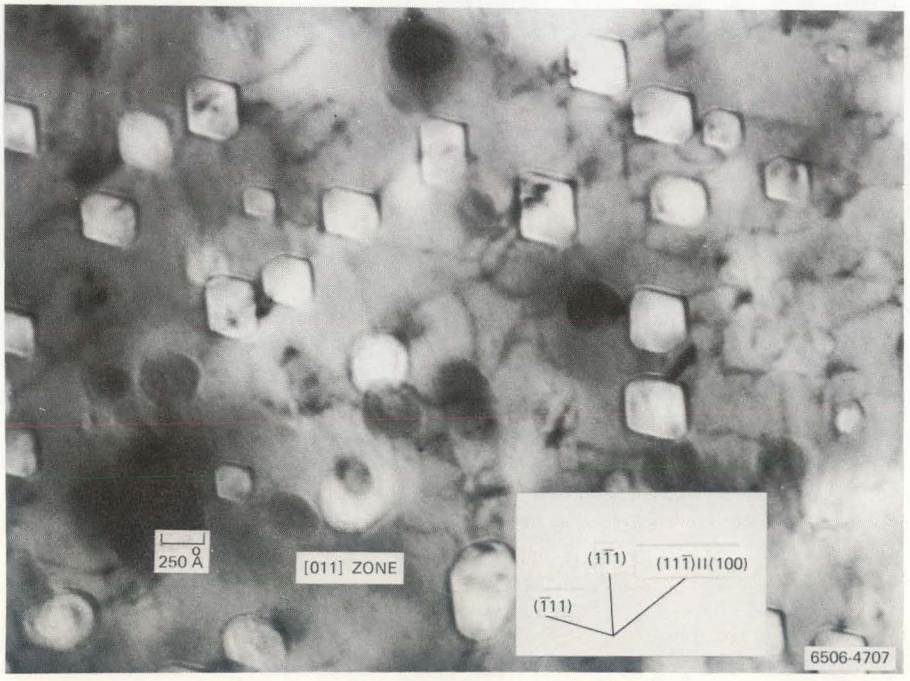

Figure 10. Transmission Electron Micrograph Showing Voids to be Octahedra Bounded by {111} Planes. Proton penetration depth >0.0076 mm.

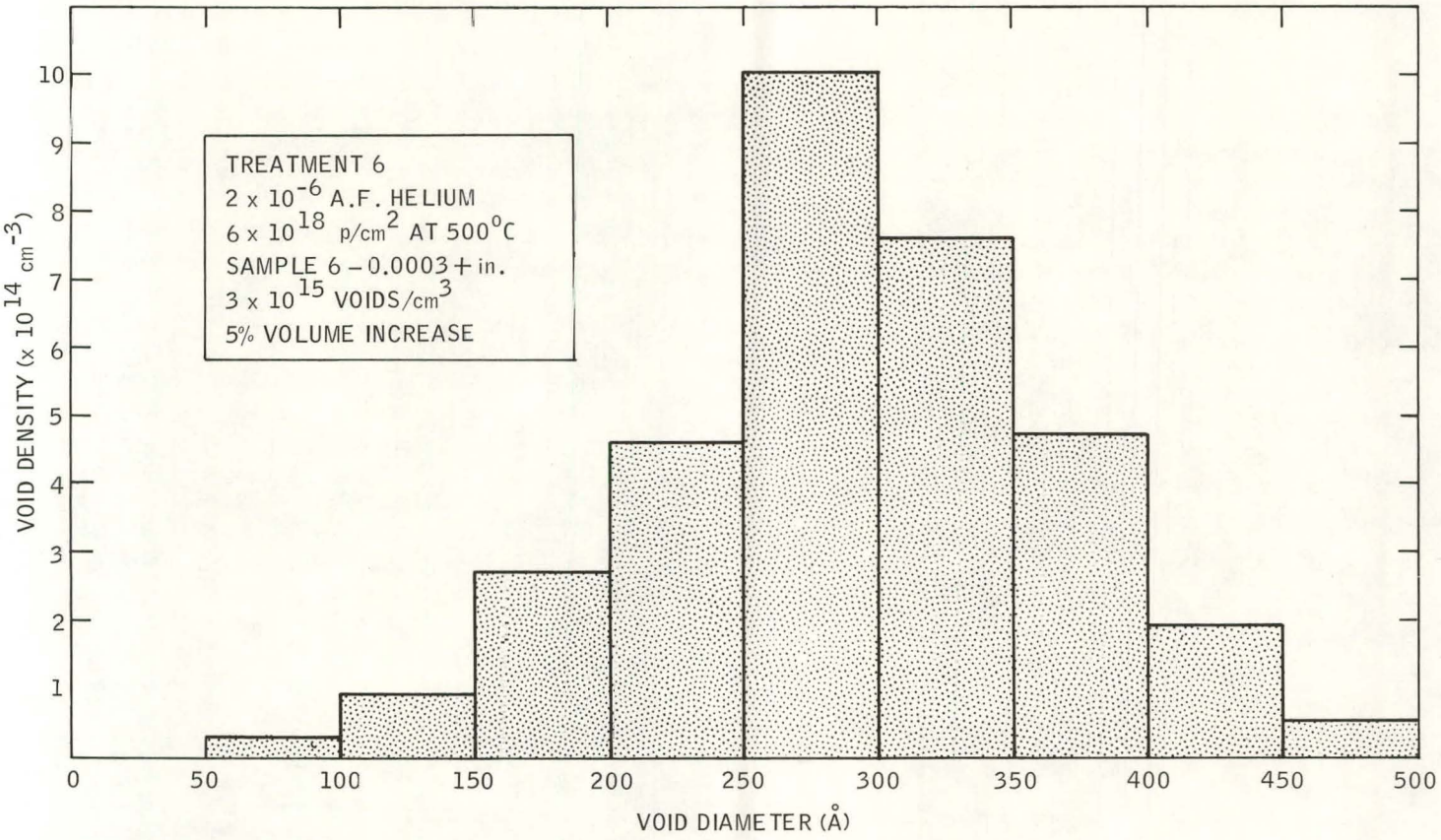

9-N25-114-29

Figure 11. Histogram Showing Void-Size Distribution at a Depth Beyond 0.0076 mm. Average void size ~290 Å.

shown that the voids are octahedra bounded by {111} planes. Occasional truncation by {100} planes was observed. This is shown in Figure 10. The void size distribution is shown in Figure 11, where the average void diameter is 290 Å. The volume swelling in this final foil is then ~5%.

IV. DISCUSSION

The production of voids in Type 316 stainless steel by proton irradiation has been amply demonstrated in this work. Although the results are preliminary, some interesting features have already emerged. In addition to voids, faulted dislocation loops, presumably of the interstitial type, were observed. Also formed during the irradiation were small precipitates which are evidently associated with dislocations in every case. The particles are too small to be identified by means of electron diffraction. The absence of a zone denuded of voids about grain boundaries in this work may be due to the higher displacement rate than is the case in reactor irradiations.

The average void size, and hence the volume swelling, increased generally with increasing depth into the specimen. This increase in void size is attributable to the increase in vacancy production, by a factor of $\sim$10, over the proton range investigated here. On the other hand, within the limits of present accuracy, the void density appeared approximately constant along the pathlength of the protons. This result provides interesting points for speculation on the nucleation process. In terms of the concept of nucleation by random encounters of diffusing vacancies, it appears that nucleation might occur very early in the irradiation. Once the even distribution of nuclei, perhaps stabilized by helium, has been established at short times, vacancies would be drained to these nuclei rather than participating in additional nucleation. This could be true in any part of the specimen, regardless of the vacancy production rate. A second possibility is that vacancy traps, such as impurities, might be distributed uniformly throughout the metal lattice. Void nuclei could form at these traps. As a third possibility, it is interesting to note that, over the proton energy range achieved here, the number of displacement spikes containing clusters of ten or more vacancies[8] is relatively constant – within a factor of two. This, of course, suggests the possibility of such clusters serving as void nuclei. It is hoped that continued work of the type presented here will assist in arriving at more detailed information on void nucleation and growth processes.

REFERENCES

1. C. Cawthorne and E. J. Fulton, Nature, 216 (1967) p 575

2. J. J. Holmes, J. Nuc. Mat., 29 (1969) p 241

3. J. L. Brimhall and B. Mastel, J. Nuc. Mat., 29 (1969) p 123

4. R. S. Nelson and D. J. Mazey, Proceedings IAEA Symposium on Radiation Damage in Reactor Materials, Vol. 2, Vienna, 1969, p 157

5. D. Kramer, H. R. Brager, C. G. Rhodes, and A. G. Pard, J. Nuc. Mat., 25 (1968) p 121

6. H. Farrar IV and C. H. Knox, American Nuclear Society, 11 (1968) p 503

7. J. F. Janni, "Calculations of Energy Loss, Range, Pathlength, Straggling, Multiple Scattering, and the Probability of Inelastic Nuclear Collisions for 0.1 to 1000 MeV Protons," AFWL-TR-65-150 (September 1966)

8. J. R. Beeler, Phy. Rev., 150 (1966) p 470